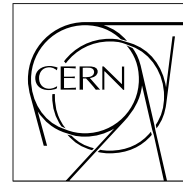


The Compact Muon Solenoid Experiment  
**Detector Note**



The content of this note is intended for CMS internal use and distribution only

02 September 2008 (v3, 19 December 2008)

# Clusters containment corrections using ECAL position measurements at the 2006 H4 testbeam

P. Meridiani<sup>a)</sup>, C. Rovelli<sup>b)</sup>

*a) CERN, Geneve, Switzerland*

*b) Università di Roma 'La Sapienza' and INFN Roma1, Roma, Italy*

## Abstract

The energy response of the CMS ECAL barrel is strongly dependent on the incidence position of the particles on the crystals. Containment effects are here investigated using the data collected during the 2006 ECAL H4 testbeam. A set of functions to correct for the changes in the containment with the position is computed and the effect on the energy resolution is discussed.

# 1 Introduction

The CMS [1] electromagnetic calorimeter (ECAL) [2] is a homogeneous calorimeter made of lead tungstate scintillating crystals. The ECAL barrel extends up to the pseudorapidity  $\eta = \pm 1.479$  and consists of 36 supermodules made of  $85 \times 20$  crystals, each one divided into 4 modules separated by 6 mm gaps. The crystals are quasi-projecting, with a 3 degrees angle between the principal axes and the line coming from the nominal vertex position both in  $\eta$  and  $\phi$ .

In summer 2006, nine supermodules were exposed to an electron beam at the H4 beam line at CERN. The final versions of the readout electronics, high and low voltage supply systems, cooling system, temperature and laser monitoring, data acquisition and data quality monitoring were tested. The supermodules were mounted on a rotating frame reproducing the same almost pointing geometry of CMS. Four planes of hodoscopes were used to reconstruct the trajectories of the electrons impinging on the crystals.

ECAL is designed to provide a precise energy and position resolution in a large range of momenta. The energy reconstructed in a cluster of crystals depends on the impact position of the impinging particle due to the changes in the energy containment. This affects the resolution which can be achieved. In this note the containment dependence on the impact position is studied with matrices of NxN crystals and a method to correct for it using the position informations provided by ECAL itself is proposed. The results obtained on testbeam data are also compared to the simulation.

## 2 Overview of the correction procedure

The energy reconstructed in a cluster of ECAL crystals depends on the impact point of the particle originating the shower on the seed crystal of the cluster. This containment effect is mainly due to the ECAL geometry and it has been deeply studied in the past, both in the full CMS setup and in dedicated testbeam analyses. In CMS the energy of electrons and photons will be reconstructed summing the energy deposits in clusters of crystals, therefore a correction for this containment effect has to be applied to obtain the design energy resolution.

At the testbeam the containment effects can be usefully investigated with fixed shape matrices of NxN crystals. A method which exploits the ratio of the energies contained in side rows or columns of crystals to the energy in the remaining part of the matrix has been proposed since long [3]. Such a technique (' $\ln E_2/E_1$ ' in the following) was extensively validated using testbeam data [4] [5] [6] and it was shown to well work to compute the needed corrections.

In this note we propose a slightly different procedure, based on the log-weighting algorithm to reconstruct the position of the particles impinging on the calorimeter [7]. The particle position in the CMS frame can be reconstructed with an energy weighted average of the positions of the crystals involved by the shower

$$\vec{X}_{CMS} = \sum_i w^i \vec{X}_{CMS}^i / \sum_i w^i \quad (1)$$

In the previous formula we called  $\vec{X}_{CMS}$  the position of the shower centre of gravity. Since the ECAL crystals are quasi-projective (Fig.1, left) the  $\vec{X}_{CMS}^i$  values depend on the depth at which the shower position is computed and here the depth  $t_{max}$  corresponding to the longitudinal centre of gravity of the shower is used. The latter varies with the beam energy according to the logarithmic law  $t_{max} = X_0(\ln E + A_0)$ , being  $X_0$  the lead tungstate radiation length (0.89 mm) and  $A_0$  a parameter which determines the overall bias. The shower density falls exponentially with the distance from the shower axis and to account for this logarithmic weights  $w_i = w_0 + \ln(E_i/E_{tot})$  are used, being  $E_{tot}$  the total energy of the cluster. Since negative weights are not included in the sum,  $w_0$  controls the smallest energy fraction a crystal can have to be considered. In the following the position is reconstructed using the energy deposited in the crystals belonging to a 3x3 matrix around the crystal with the largest energy deposit and the values  $A_0 = 7.4$  and  $w_0 = 5$  are used. More details on the choice of the parameters can be found in [8]. The final reference frame is chosen with the  $Z_{ECAL}$  axis parallel to the beam line, so that  $(X_{ECAL}, Y_{ECAL})$  are parallel to the hodoscope reference frame, hence giving the possibility to compare ECAL and hodoscope reconstructed positions. A sketch defining better the final reference frame is shown in Fig.1, right.

For the correction procedure we discuss here, the energy deposited in a 3x3 or 5x5 array of crystals is studied as a function of the impact position reconstructed with the log-weighting method. The data are divided in bins of the reconstructed X (Y) and a Crystal Ball function is fitted to the measured energy in each bin. The mean of the fit is evaluated as a function of the reconstructed position. Finally, polynomial fits are performed independently in the two coordinates to compute the correction functions. In this way, the knowledge of the beam position with external devices is not required.

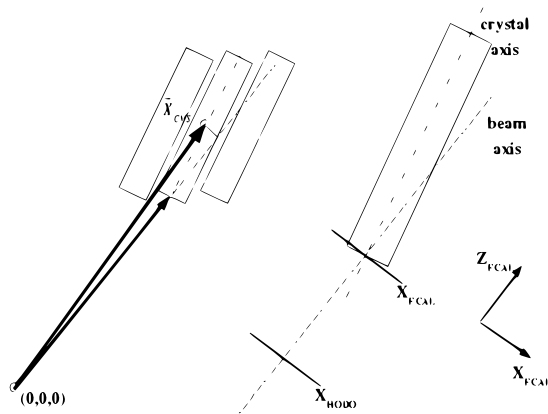


Figure 1: Position reconstruction procedure based on calorimetric informations. First the particle position is reconstructed in the CMS frame with an energy weighted average of the positions of the crystals involved by the shower (left). Then it is rotated in a reference frame compatible with the hodoscope reference one (right), with the  $Z_{ECAL}$  axis parallel to the beam line and  $(X_{ECAL}, Y_{ECAL})$  parallel to hodoscopes.

### 3 Correction curves

The study discussed here is based on the data collected at the 2006 H4 ECAL testbeam. Dedicated large statistics samples collected at different energies on SM22, SM18 and SM16 were analyzed together with the intercalibration runs taken on some of the available supermodules. To compute the corrections in the X (Y) direction only electrons impacting in a  $\pm 2$  mm region (measured with the hodoscopes) around the point of maximum containment in Y (X) are considered. The crystal under analysis is always required to be the one with the largest energy deposit. The amplitude in the crystals is evaluated using the weight method [9], with optimized weights calculated from a shape profile specific for each crystal when available [10]. The intercalibration coefficients computed using the S1 method [11] are used.

The normalized energy in matrices of 3x3 and 5x5 crystals around the crystal with the maximum energy deposit is shown in Fig.2 as a function of the reconstructed position ( $X_{ECAL}$  and  $Y_{ECAL}$ ). Each point is obtained

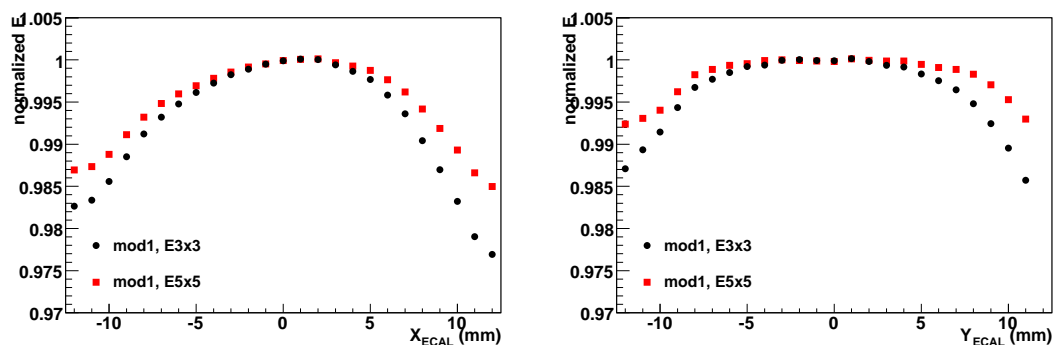


Figure 2: Normalized energy in 3x3 and 5x5 matrices around the crystal under analysis as a function of the reconstructed impact position. The 25 crystals belonging to the trigger tower 11 in SM22 are analyzed and averaged. The crystal under analysis is always required to be the one with the largest energy deposit. The X (Y) coordinate is shown on the left (right).

analyzing 3 runs in each direction, one with the beam pointing to the crystal centre and the others to the two crystal

edges in the direction under analysis. Since the curves obtained for crystals close to each other are very similar the data collected on the 25 crystals of one same trigger tower are here always averaged to reduce the statistical fluctuations. The plots in Fig.2 refer to trigger tower 11 in Mod1, SM22. Some general trends which are common to all the analyzed crystals can be seen:

- in both X and Y the corrections at the crystal edges are  $\sim 0.5\%$  larger for the sum of 9 crystals with respect to the sum of 25
- in the 3x3 case an asymmetry between the two crystal edges is largely visible which is much reduced when a 5x5 matrix is used [4]. This asymmetry is due to the tilt of the crystals and it is well reproduced by the simulation
- the corrections are larger in X than in Y. This effect, which is not reproduced by the simulation, is  $\sim 0.5\%$

Similar considerations also holds in the case of the  $\ln E_2/E_1$  method.

### 3.1 Containment dependence on the beam direction

In Fig.3 we compare the results obtained using three runs directed as discussed in the previous section and one single run with the beam pointing to the crystal centre. The comparison is shown for crystals in Mod1 and Mod4. In both cases the curves are compatible, with only minor differences at the crystal edges.

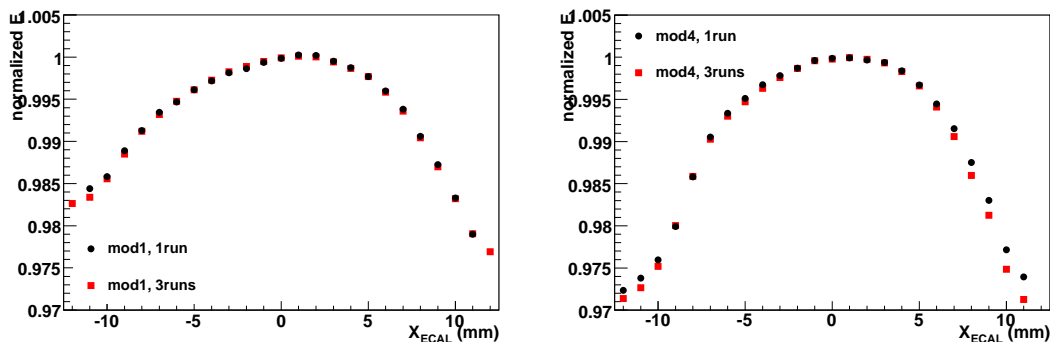


Figure 3: Normalized energy in a 3x3 matrix around the crystal under analysis as a function of the reconstructed impact position in the X direction. Squared dots are the result of an analysis performed on 3 runs, with the beam pointing to the centre and the edges of the crystal; round dots correspond to the central run only. In both cases the crystal under analysis is required to be the one with the largest energy deposit. The crystals belonging to (left) trigger tower 11 (SM22) and (right) trigger tower 61 (SM18) are analyzed.

This good agreement allows to use intercalibration runs (taken at the crystal centre only, using the  $20 \times 20 \text{ mm}^2$  trigger) to extend the analysis to more supermodules. In addition we require the maximum energy crystal to be the crystal struck by the beam. This requirement is applied from now on to obtain the final correction curves; the hodoscope information is used to restrict the analysis to a small region in the direction not under study.

### 3.2 Containment dependence on the beam energy

Fig.4 compares the cluster containment dependence on the impact position at different energies both for a 3x3 and 5x5 array of crystals. The curves refer to the average of 25 crystals in trigger tower 10 of SM16. The data collected have been analyzed up to 150 GeV. There is no clear trend in the shape of the curves, but there is a small monotonic shift in X. The size of this is consistent with the change in the depth of the shower maximum with energy, leading to a shift in the projected X-coordinate of the order of  $\sim 1 \text{ mm}$ . The resulting energy dependence of the containment factors is negligible for the purpose of this work. In the following we therefore apply the same corrections computed at 120 GeV to all the energies.

### 3.3 Containment dependence on the crystal position within the supermodule. Comparison between supermodules

To be usefully exploited during the data taking, only a small number of correction curves has to be computed to be applied to the full ECAL barrel and also to the supermodules not analyzed at the testbeam. In this section the

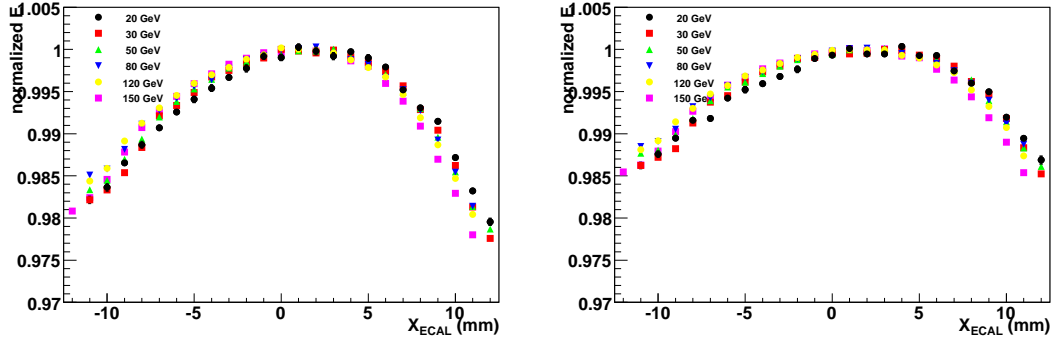


Figure 4: Normalized energy in a 3x3 (left) or 5x5 (right) matrix around the crystal under analysis as a function of the reconstructed impact position in the X direction. Data with beam energies between 20 GeV and 150 GeV are compared. The crystals belonging to trigger tower 10 (SM16) are analyzed and their behaviours averaged. The crystal under analysis is always required to be the one with the largest energy deposit. It is also required to be the one struck by the beam. Only electrons impacting within  $\pm 2mm$  with respect to the point of maximum containment in the Y direction are considered.

generality of the corrections is investigated through the study of the dependence on the crystal position within the supermodule. Also, the results obtained for different supermodules are compared.

To scan the whole supermodule, intercalibration runs were used and crystals belonging to the same trigger tower were analyzed together to increase the statistics. The crystals close to the module boundaries were excluded by the analysis. In Fig.5 we compare the curves computed at different positions in  $\phi$  on a reference supermodule, for

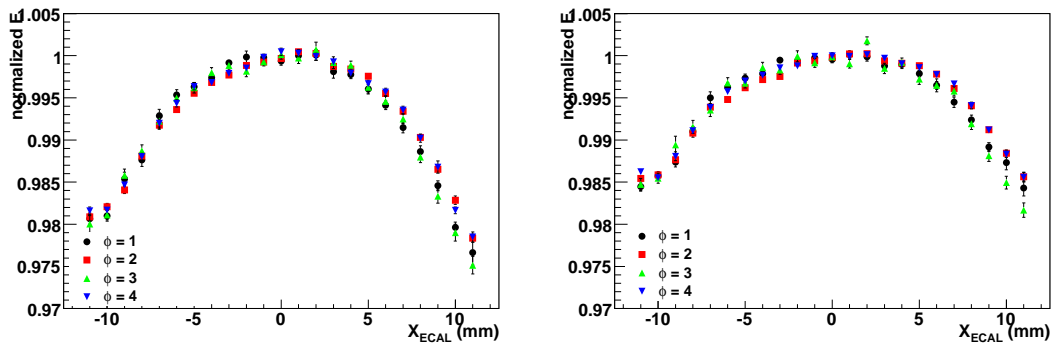


Figure 5: Normalized energy in a 3x3 (left) or 5x5 (right) matrix around the crystal under analysis as a function of the reconstructed impact position in the X direction. Crystals at different  $\phi$  in the supermodule are compared. Each graph corresponds to a trigger tower for crystals of type 12 in SM16. The crystal under analysis is always required to be the one with the largest energy deposit. It is also required to be the one struck by the beam. Only electrons impacting within  $\pm 2mm$  with respect to the point of maximum containment in the Y direction are considered.

crystals of type 12 (module 3) as an example. We define  $i\phi$  ( $i\eta$ ) the position in  $\phi$  ( $\eta$ ) in units of crystals. In the plots,  $\phi = 1$  refers to crystals with  $i\phi = 1, 2, 3, 4, 5$  in the testbeam view and so on up to  $\phi = 4$  for  $i\phi = 16, 17, 18, 19, 20$ . As expected, the energy loss is almost independent on the position in  $\phi$  of the crystal in the supermodule and even for electrons impacting close to the crystal edges the results at different  $\phi$  well compare. In Fig.5 the maximum spread is about 3 permill for both the 3x3 and the 5x5 analysis. This difference ranges between 0.1% and 0.5% considering all the pseudorapidities and supermodules, both in X and Y. On the basis of the results shown here the same correction is expected to hold for all the  $\phi$  values and the data are therefore integrated in  $\phi$  in the following of this analysis.

Due to the increasing staggering of the crystals with the pseudorapidity, a dependence of the containment on the position in  $\eta$  of the crystal in the supermodule is expected. Fig.6 and Fig. 7 compare the containment corrections in X and Y on the 3x3 computed at different positions in  $\eta$  on a reference supermodule after the integration in  $\phi$ ; similar results are found in the 5x5 analysis also and on other supermodules. Moving from M1 to M4 the change in the containment in X is up to 1.5%, the effect being visible mainly at high pseudorapidities. In Y the differences

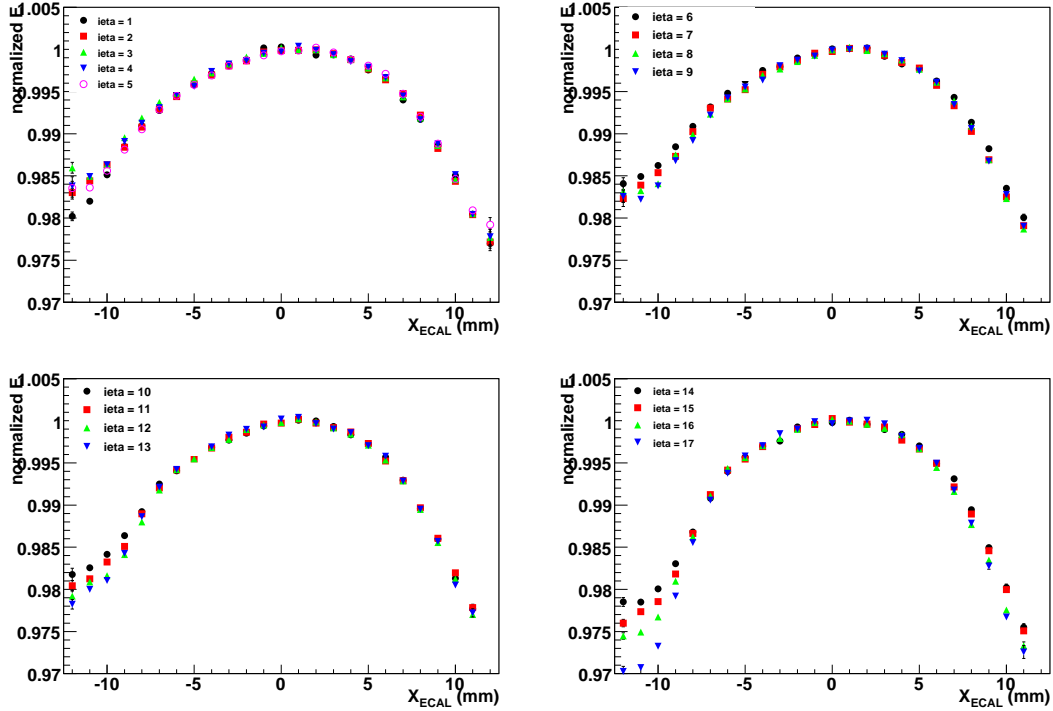


Figure 6: Normalized energy in a 3x3 matrix around the crystal under analysis as a function of the reconstructed impact position in the X direction. Crystals at different pseudorapidities in the supermodule are compared separately for the four ECAL barrel modules. Each graph corresponds to the integral of the four trigger towers at the given  $\eta$  in SM17. The crystal under analysis is always required to be the one with the largest energy deposit. It is also required to be the one struck by the beam. Only electrons impacting within  $\pm 2mm$  with respect to the point of maximum containment in the Y direction are considered.

are reduced to about 0.5%-0.7%. We computed one correction function per each module. The effect of this choice on the energy resolution which can be obtained will be addressed in the following sections to quantify the necessity of having different corrections for different pseudorapidities.

Finally, as mentioned at the beginning of this section, the same correction has to be applied to all the barrel supermodules. In Fig.8 we compare the correction curves after the integration in  $\phi$  for the 5 supermodules which were intercalibrated with a 120 GeV beam (SM 6, 16, 17, 18, 22). The agreement among the different supermodules is between 0.1% and 0.5% at each pseudorapidity (here crystals of type 12 are shown); no explanation has been found for the residual discrepancy, which is anyway small. Since dedicated corrections can not be computed for each supermodule, in the following we integrate all the data to establish an average correction.

## 4 Comparison with the simulation

The results obtained on testbeam data have been compared to the Montecarlo. The full ECAL simulation implemented in the CMSSW framework and based on Geant4 has been used [12]. The results discussed here refer to the final simulation of the testbeam setup in which a detailed description of the materials along the beam line is also included; data were produced using the CMSSW\_2\_1\_0 version of the framework with the QGSP physics list. We produced 30k events/crystal for the same crystals in Mod.1 used for the SM16 data analysis. Simulation and real data are compared in figure 9 for the X and Y direction and for the average sum of 9 and 25 crystals around each crystal under analysis. As for the data, in the simulation also the effect is much reduced for the sum of 25 crystals with respect to the sum of 9. In X the correction is  $\sim 0.5\%$  larger in the data than in the simulation, the opposite happens in Y. The 0.5% differences seen in data between X and Y is not reproduced by the simulation. To investigate the possibility of a bad description of gaps between crystals we used a modified version of the testbeam setup in which we changed the relative positions of the crystal centers. The results are given in Appendix A.

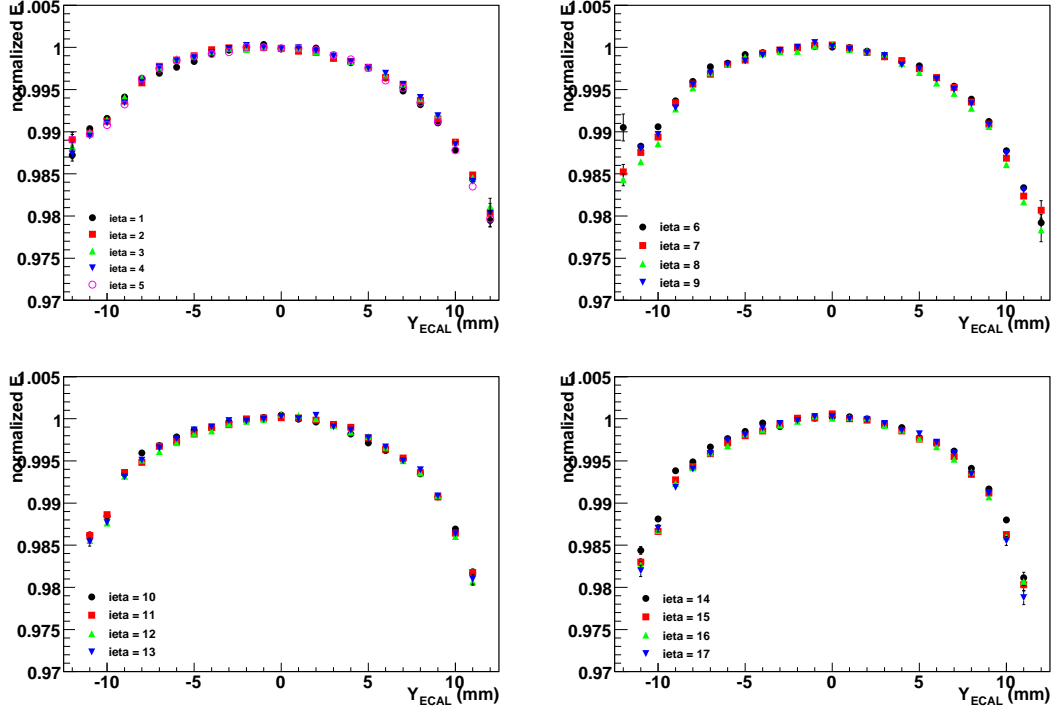


Figure 7: Normalized energy in a 3x3 matrix around the crystal under analysis as a function of the reconstructed impact position in the Y direction. Crystals at different pseudorapidities in the supermodule are compared separately for the four ECAL barrel modules. Each graph corresponds to the integral of the four trigger towers at the given  $\eta$  in SM17. The crystal under analysis is always required to be the one with the largest energy deposit. It is also required to be the one struck by the beam. Only electrons impacting within  $\pm 2mm$  with respect to the point of maximum containment in the X direction are considered.

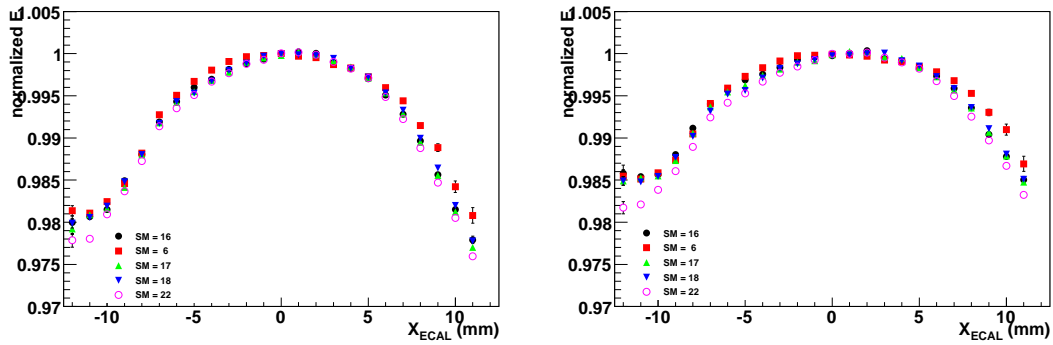


Figure 8: Normalized energy in a 3x3 (left) or 5x5 (right) matrix around the crystal under analysis as a function of the reconstructed impact position in the X direction. Results on 5 different supermodules are compared. Crystals of type 12 after an integration in  $\phi$  are shown. The crystal under analysis is always required to be the one with the largest energy deposit. It is also required to be the one struck by the beam. Only electrons impacting within  $\pm 2mm$  with respect to the point of maximum containment in the Y direction are considered.

## 5 Effect of the correction procedure on the energy resolution

In the previous sections the containment dependence on the crystal position in the supermodule has been investigated, together with the agreement between different supermodules. As discussed above, we computed 4 correction curves for the X direction and 4 for Y, using all the data collected on 5 analyzed supermodules and dividing them by modules.

In Fig.10 we show the energy reconstructed in the 3x3 and 5x5 matrices around the crystal under analysis after

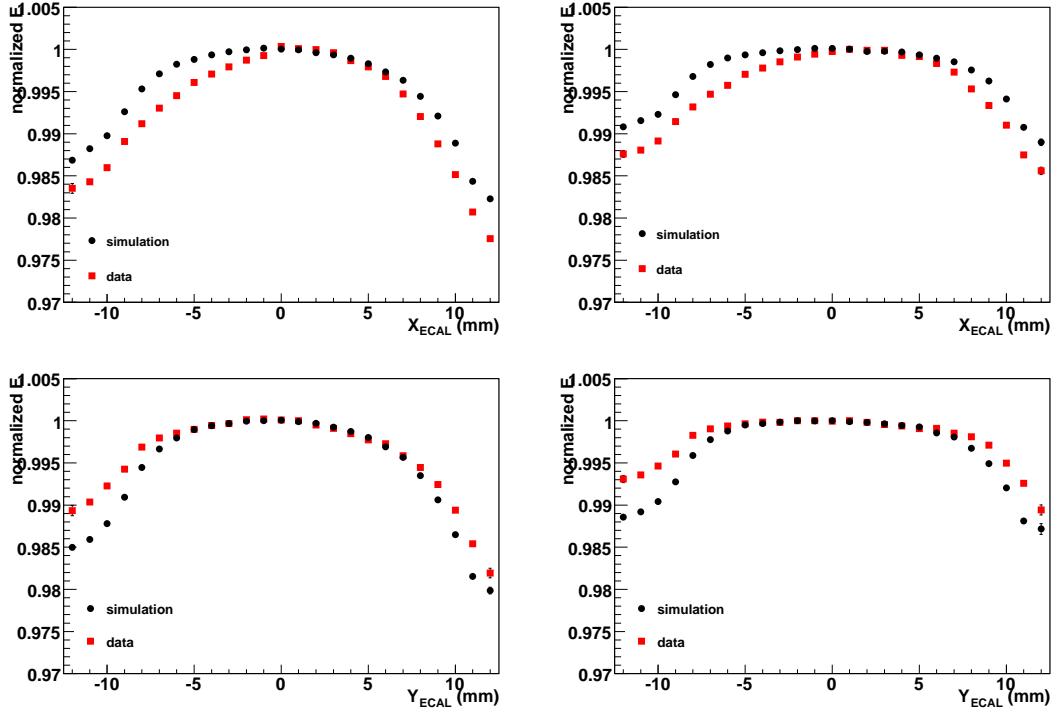


Figure 9: Normalized energy in a 3x3 (left) or 5x5 (right) matrix around the crystal under analysis as a function of the reconstructed impact position in the X (top) and Y (bottom) direction. Data collected on the crystals belonging to trigger tower 10 (SM16) are compared with simulated data on the same crystals. The crystal under analysis is always required to be the one with the largest energy deposit. It is also required to be the one struck by the beam. Only electrons impacting within  $\pm 2mm$  with respect to the point of maximum containment in the direction not under analysis are considered.

the correction as a function of the impact point in X. We also compare the energy distribution before and after the correction. The plots refer to crystal 287 in SM16 taken as an example on which the average correction computed for module 1 was applied. Here the crystal under analysis is required to be the maximum amplitude one, but the requirement about the crystal hit by the beam is removed since it can not be applied in CMS. The functions computed integrating data collected in a large area seem to work fine and they can be used to correct the single crystal response. Similar considerations also hold for the other crystals analyzed within differences of few permills.

To quantify the performance of the corrections, the effect on the energy resolution has been studied in trigger tower 10 on SM16. We want to stress here that the distributions which follow are not supposed to be a full estimate of the ECAL energy resolution but they should be used as a test of the correction procedure only. The reconstructed energies in a 3x3 or a 5x5 matrix were computed for each of the 25 crystals of the trigger tower using optimized weights and they were summed after a rescaling to place the peak of each distribution at the beam energy. In Fig. 11 we show such distributions at 120 GeV, with superimposed the result of a fit with a Crystal Ball function. The energy resolution is  $0.43 \pm 0.01\%$  both for an array of 3x3 and of 5x5 crystals; the quoted error also includes an estimate of the systematics of the fit. Since the distributions for the single crystals were rescaled before summing them up the result does not include the contribution of intercalibration (which was found to be order of 0.2% at the testbeam) but it accounts for a larger crystals statistics with respect to a single crystal analysis. This result well compares with the 2004 testbeam one [4], obtained on one single crystal.

The case of uniform impact of the beam on the crystal was reproduced with a reweighting of the events to make the beam profile flat in the region (-13 mm, +13 mm) measured by hodoscopes. Since the hodoscope position was available with respect to the crystal hit by the beam only, only those events in which the latter was really the maximum amplitude one were retained for the analysis. The corresponding distributions are shown in figure 12; at 120 GeV the deterioration of the resolution corresponds to an additional term of about 0.15% when the beam reweighting is applied. In figure 13 the distributions in the X-Y plane of the events entering the analysis before and after the reweighting of the events are shown to quantify the reweighting effect. Finally, the energy resolution for central incidence is given as a reference not affected by containment effects in figure 14; central incidence is here defined as incidence within  $4 \times 4 \text{ mm}^2$  around the maximum containment point. The three curves are compared

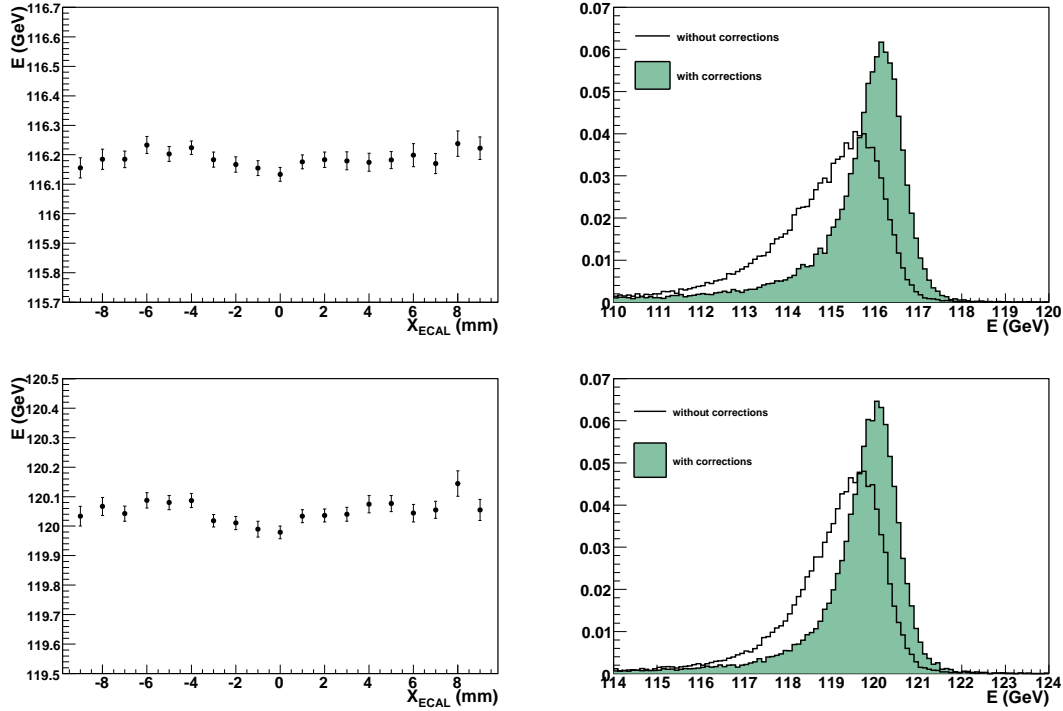


Figure 10: Left: energy reconstructed in a 3x3 (top) or a 5x5 (bottom) matrix around the crystal under analysis as a function of the reconstructed impact position in the X direction. Data refer to crystal 287 in SM16 which is required to be the crystal with the largest energy deposit. Right: energy reconstructed in a 3x3 (top) or a 5x5 (bottom) matrix around crystal 287 before and after the correction for the containment effect.

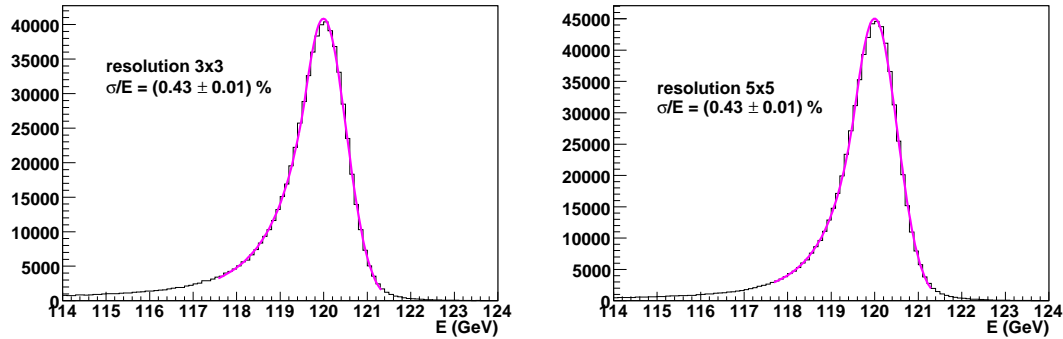


Figure 11: Left: energy reconstructed in a 3x3 (left) or a 5x5 (right) matrix around 25 different crystals for 120 GeV electrons after the correction for containment effects. Data refer to trigger tower 10 in SM16. A rescaling to place the peak of the distribution to the beam energy is applied. Superimposed is the result of a fit with a Crystal Ball function.

as a function of the beam energy in figure 15. At high energy, the difference in quadrature between the central incidence case result and the one related to the uniform impact case with the containment correction is  $\sim 0.2\%$ .

Last, in order to establish if one correction is enough for the full supermodule we computed the energy resolution using correction functions determined on the average of crystals in other modules with respect to the one under analysis. The result of the fits are compared in figure 16 on the left for Mod.1 crystals and on the right for Mod.4. For module 4, data collected in SM6 were analyzed, but it must be stressed that their quality was found to be not good in many other parallel analyses, therefore we suggest to use these numbers just as a relative comparison and not as absolute values. The resolution is degraded by 0.15%-0.3% using corrections computed on the ‘wrong’ module. The effect is larger for module 1, where the resolution is intrinsically better. Detailed results are given in

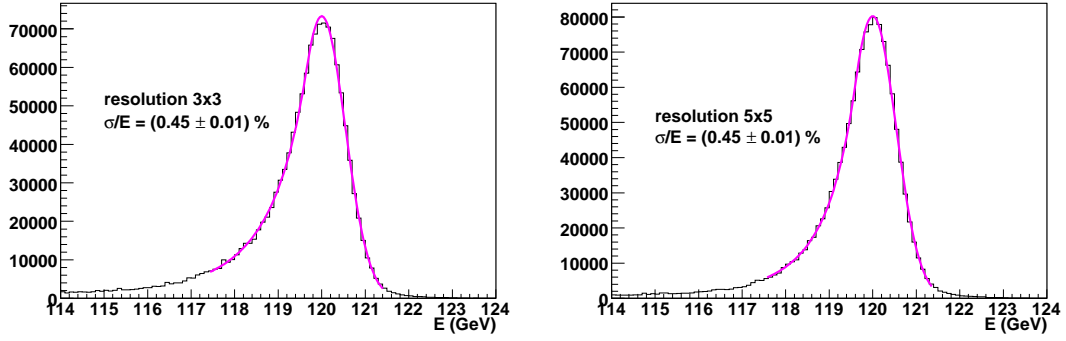


Figure 12: Left: energy reconstructed in a 3x3 (left) or a 5x5 (right) matrix around 25 different crystals for 120 GeV electrons after the correction for containment effects and an event reweighting to emulate uniform impact on the crystal. Data refer to trigger tower 10 in SM16. Superimposed is the result of a fit with a Crystal Ball function. A rescaling to place the peak of the distribution to the beam energy is applied.

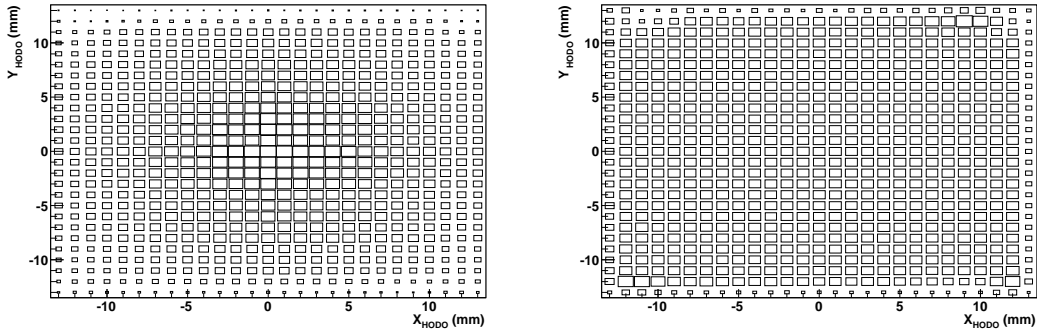


Figure 13: Distribution in the X-Y plane of the of the events selected for the standard analysis (left) and after the reweighting of the events to emulate the uniform impact condition.

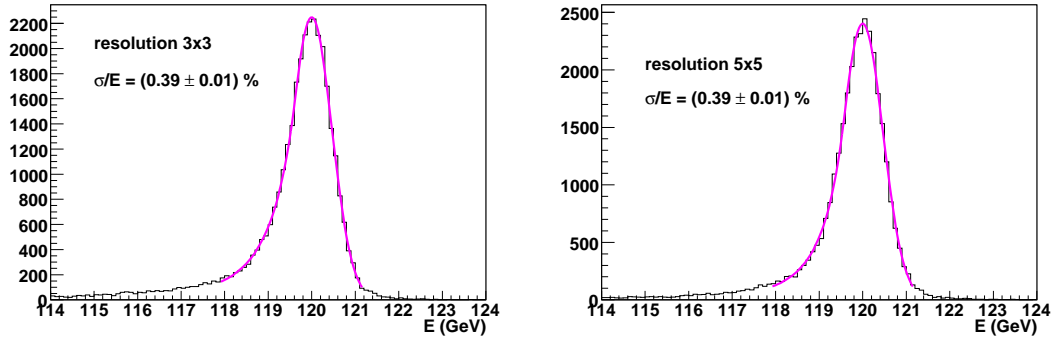


Figure 14: Left: energy reconstructed in a 3x3 (left) or a 5x5 (right) matrix around 25 different crystals for 120 GeV electrons. Only central impacting electrons (within 4x4 mm<sup>2</sup> around the maximum containment point) are used. Data refer to trigger tower 10 in SM16. Superimposed is the result of a fit with a Crystal Ball function. A rescaling to place the peak of the distribution to the beam energy is applied.

table 1. From these numbers, it seems that a good compromise between generality and precision could be to use four corrections, computed on each of the four modules.

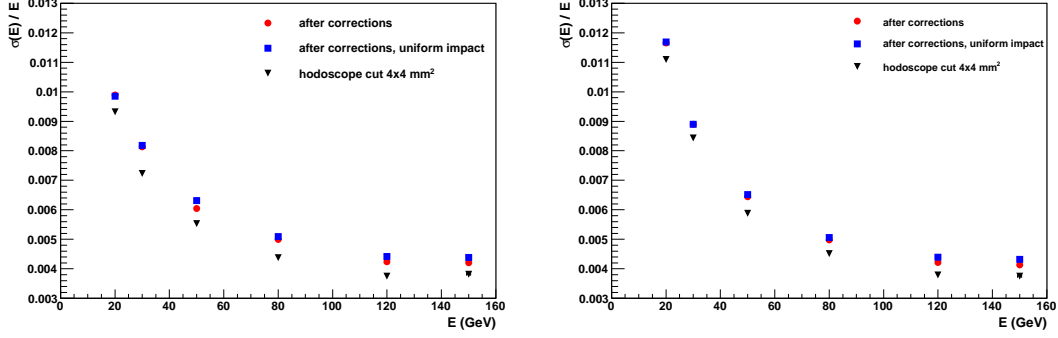


Figure 15: Energy resolution as a function of the beam energy for a 3x3 (left) and a 5x5 (right) array of crystals. The resolution for central incidence (black triangles) and after the containment corrections without (red) and with (blue) beam reweighting are compared. Data refer to trigger tower 10 in SM16.

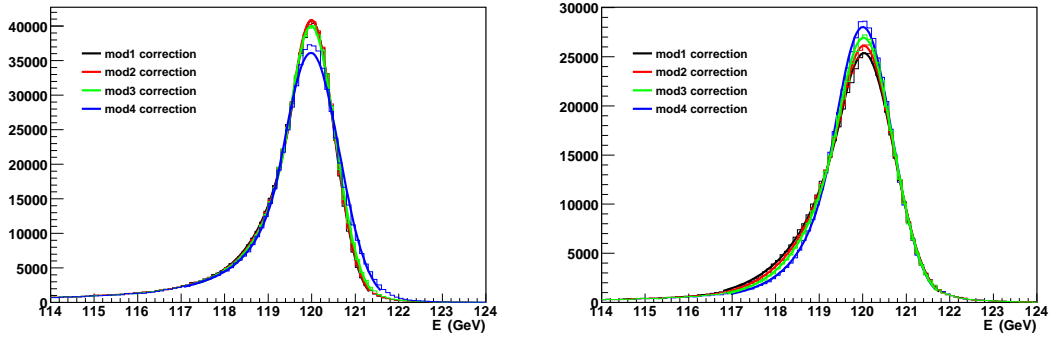


Figure 16: Energy reconstructed in a 3x3 array around 25 different crystals in Mod1 SM16 (left) and Mod4 SM6 (right) for 120 GeV electrons after the correction for containment effects. Four different functions computed on the 4 modules are used to correct and compared. Superimposed is the result of fits with a Crystal Ball function. A rescaling to place the peak of the distribution to the beam energy is applied.

	Mod.1 correction	Mod.2 correction	Mod.3 correction	Mod.4 correction
Mod.1 data	$(0.43 \pm 0.1)\%$	$(0.44 \pm 0.1)\%$	$(0.46 \pm 0.1)\%$	$(0.53 \pm 0.1)\%$
Mod.4 data	$(0.70 \pm 0.1)\%$	$(0.69 \pm 0.1)\%$	$(0.69 \pm 0.1)\%$	$(0.67 \pm 0.1)\%$

Table 1: Energy resolution at 120 GeV obtained fitting with a Crystal Ball function a 3x3 matrix around 25 different crystals in Mod.1 (top) and Mod.4 (bottom). Functions computed on crystals belonging to Mod.1, Mod.2, Mod.3, Mod.4 are used to compute the containment corrections.

## 6 Conclusions

We exploited the log-weighting method for the particles position reconstruction to correct for the position dependence of the energy in a crystal cluster. The effect was found to be reproducible within few permills for different beam energies and crystal positions in the supermodule. A good agreement between the supermodules was found. After the correction, the energy resolution well compares with the case of central incidence.

## 7 Acknowledgments

We wish to thank Brian Heltsley for the precious help in the study of the simulation geometry changes. Thanks to the ECAL Editorial Board members for the very useful comments on the draft of this note.

## References

- [1] CMS Collaboration, ‘The Compact Muon Solenoid - Technical Proposal’, CERN/LHCC 94-38 (December 1994).
- [2] CMS Collaboration, ‘The Electromagnetic Calorimeter Project - Technical Design Report’, CERN/LHCC 97-23 (December 1998) 290pp.
- [3] A.Givernaud and E.Locci, ‘Study of the Azimuthal Cracks in the Electromagnetic Calorimeter: the Photon Case’, CMS TN 1996/014
- [4] J.Descamps and P.Jarry, ‘Periodic position dependence of the energy measured in the CMS electromagnetic calorimeter’, CMS Note 2006/045
- [5] A.Kyriakis, A.Markou and E.Petrakou, ‘Position Dependence of Energy Containment in ECAL Barrel Crystals’ CMS DN 2007/017
- [6] E.Locci, ‘Energy measurement in CMS ECAL using test-beam data’ CMS DN 2008/005
- [7] E.Meschi et al, ‘Electron Reconstruction in the CMS Electromagnetic Calorimeter’, CMS IN 2001/034
- [8] P.Meridiani and C.Rovelli, ‘Position resolution at the 2006 ECAL testbeam’ CMS DN 2007/011
- [9] C.Baty et al, ‘Amplitude reconstruction and basic performance of the CMS electromagnetic calorimeter’, CMS DN 2007/008
- [10] C.Seez, D.Wardrope and A.Zabi, ‘CMS Electromagnetic Calorimeter: Amplitude reconstruction Using Optimized Weights’, CMS DN 2007/020
- [11] A.Benaglia et al, ‘Intercalibration at 2006 ECAL testbeam with the single crystal technique’, CMS DN 2007/001
- [12] F.Cossutti, ‘The CMS electromagnetic calorimeter simulation’, CMS CR 2006/093

## A Appendix: Simulation studies

To better understand the comparison between data and simulation we studied the impact of a possible change of the gap between the crystals in the supermodule geometry. We simulated an ‘expanded’ and ‘compactified’ supermodule by changing the thickness of the alveola between the crystals from the default value ( $120\ \mu\text{m}$ ) to  $20\ \mu\text{m}$  and  $220\ \mu\text{m}$ . The crystals dimensions are not affected by these changes.

We generated a  $120\ \text{GeV}$  electron beam pointing to the centre of crystal 248. The energy reconstructed in a  $3\times 3$  matrix as a function of the position read by the hodoscopes in the X coordinate is shown in figure 17. The results

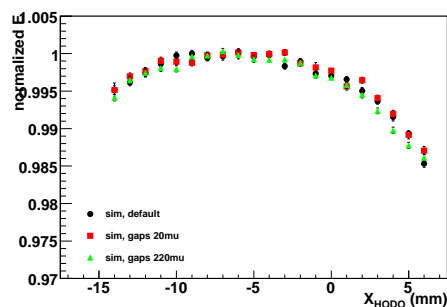


Figure 17: Simulated normalized energy in a  $3\times 3$  matrix around crystal 248 as a function of the impact position of the electron measured with hodoscopes in the X direction. The default simulation of the supermodule is compared with modified ones in which the thickness of the alveola between the crystals is changed from the default value ( $120\ \mu\text{m}$ ) to  $20\ \mu\text{m}$  and  $220\ \mu\text{m}$ . The crystal under analysis is required to be the one with the largest energy deposit. Only electrons impacting within  $\pm 2\text{mm}$  with respect to the point of maximum containment in the Y direction are considered.

obtained with the three geometry configurations well agree among them, therefore the origin of the disagreement between data and Montecarlo can not be attributed to a wrong description of the geometry in the simulation.